Published in final edited form as:
Biochemistry. 2011 February 22; 50(7): 1135–1142. doi:10.1021/bi101915z.

Unlocking the Sugar 'Steric Gate' of DNA Polymerases†

Jessica A. Brown[‡,§] and **Zucai Suo**[‡,§,‖,⊥,@,*]

[‡]Department of Biochemistry, The Ohio State University, Columbus, OH 43210

[§]Ohio State Biochemistry Program, The Ohio State University, Columbus, OH 43210

[‖]Ohio State Biophysics Program, The Ohio State University, Columbus, OH 43210

[⊥]Molecular, Cellular & Developmental Biology Program, The Ohio State University, Columbus, OH 43210

[@]Comprehensive Cancer Center, The Ohio State University, Columbus, OH 43210

Abstract

To maintain genomic stability, ribonucleotide incorporation during DNA synthesis is controlled predominantly at the DNA polymerase level. A steric clash between the 2′-hydroxyl of an incoming ribonucleotide and a bulky active site residue, known as the 'steric gate', establishes an effective mechanism for most DNA polymerases to selectively insert deoxyribonucleotides. Recent kinetic, structural, and *in vivo* studies have illuminated novel features about ribonucleotide exclusion and the mechanistic consequences of ribonucleotide misincorporation on downstream events, such as the bypass of a ribonucleotide in a DNA template and the subsequent extension of the DNA lesion bypass product. These important findings are summarized in this review article.

Based on primary sequence similarity, DNA polymerases (Pol) are classified into one of six families: A, B, C, D, X, or Y (1-3). In addition, the reverse transcriptase (RT) family is sometimes considered to be an additional family since each RT possesses both DNA- and RNA-dependent DNA polymerase activities. DNA polymerases catalyze nucleotidyl transfer of the four natural deoxyribonucleotide 5′-triphosphates (dNTPs) during DNA replication, repair, lesion bypass, sister chromatid exchange, and antibody generation processes (4). Despite functioning in diverse cellular roles, all *in vitro* characterized DNA polymerases catalyze nucleotide incorporation using a two divalent metal ion mechanism, follow a minimal kinetic pathway, and share a similar structural architecture of the polymerase domain which is composed of the fingers, palm, and thumb subdomains (5,6). These subdomains move in response to the binding of an incoming dNTP and are thought to contribute to polymerase fidelity due to different conformational dynamics induced by correct and incorrect dNTPs (7-11). In addition, the fidelity of nucleotide incorporation is achieved mostly during two general steps of the polymerase kinetic pathway: nucleotide binding and nucleotide incorporation.

Throughout most of the cell cycle, the intracellular concentration of ribonucleotide 5′-triphosphates (rNTPs) exceeds the levels of dNTPs by 10- to 2,000-fold depending on the rNTP/dNTP pair and organism (12-14). Therefore, DNA polymerases have evolved mechanisms to restrict the misincorporation of rNTPs, substrates with an incorrect sugar,

†This work was supported by National Science Foundation Grant MCB-0960961 and National Institutes of Health Grant GM079403 to Z.S. J.A.B. was supported by a Presidential Fellowship from The Ohio State University.

*To whom correspondence should be addressed: 880 Biological Sciences, 484 West 12th Avenue, Columbus, OH 43210 U.S.A.; Telephone: +1 614 688 3706; Fax: +1 614 292 6773; suo.3@osu.edu. .

during DNA synthesis. Recently, it has been reported that *Saccharomyces cerevisiae* replicative DNA polymerases α, δ, and ε may misincorporate over 10,000 rNTPs during a single round of nuclear genomic replication in yeast (14,15). This result suggests that rNTPs may be the most common aberrant nucleotides inserted into a eukaryotic genome. In addition, following misincorporation during gap-filling DNA synthesis, rNTPs can become embedded into genomic DNA during the final ligation step in DNA repair pathways (16-18). Together, these studies highlight the biological importance of understanding the mechanisms of sugar selection employed by DNA polymerases which are the primary deterrents of rNTP incorporation into genomic DNA. This review will focus on the kinetic and structural basis of how a DNA polymerase discriminates between dNTPs and rNTPs during the incorporation, extension, and bypass processes.

MOLECULAR BASIS OF SUGAR SELECTION

Expanded steric exclusion model: either an active site residue's side chain or a protein backbone segment plays the major 'steric gate' role in steric discrimination against rNTPs

Most DNA polymerases and RTs have evolved a stringent nucleotide selection mechanism to prevent misincorporation of rNTPs into DNA (19). The rejection of rNTPs occurs via a simple steric exclusion model: an active site residue, usually one with a bulky side chain, collides with the 2′-OH group on the ribose ring of an incoming rNTP (Figure 1). To date, the amino acid residues, or 'steric gates', involved in regulating sugar discrimination include Glu for A-family polymerases (20,21) and Tyr or Phe for members of the B-, X-, Y-, and RT-families (21-31). From the aforementioned steric clash, this mechanism of discrimination between dNTPs and rNTPs has sugar selectivity values, defined as dNTP incorporation efficiency divided by rNTP incorporation efficiency, measured to be 280 to 4,400,000 using kinetic and quantitative gel-based techniques for most DNA polymerases and RTs (Table 1). The kinetic basis of inefficient rNTP incorporation is due to the weaker binding and slower rate of incorporation compared to dNTPs (20,26,28,29,31,32). In general, the incorporation step is affected more than the binding step based upon the pre-steady state kinetic parameters for insertion of a dNTP versus rNTP. However, rat Pol β, *Sulfolobus acidocaldarius* DinB homolog (Dbh), and human Rev1 do not discriminate during the nucleotide binding step, thereby suggesting the active site is not optimally assembled for the 'steric gate' residue to clash with the 2′-OH (28,32,33). Reducing the size of the side chain at the 'steric gate' position (*i.e.* from E/Y/F to V/A/G mutation) creates a DNA polymerase that incorporates matched rNTPs as efficiently as correct dNTPs, thereby leading to relatively low sugar selectivity values of 2 to 33 (Figure 2) (20,24-26,28). Thus, the side chain of a 'steric gate' residue is in closest proximity to the C2′ position which would clash with a 2′-OH of an incoming rNTP (Figures 1 and 3). This putative steric clash is modeled using the Y12 residue of DNA polymerase IV (Dpo4) and an incoming rATP (Figure 3B). Here, the Y12 residue as well as the triphosphate and adenine base of an incoming dATP were unaltered (PDB 2AGQ) while the ribose ring of rATP bound to N5-CAIR synthetase (PDB 3ETH) was used to replace the ribose of the incoming dATP in the Dpo4 crystal structure (34,35). Using SwissPDB Viewer (36), Tyr12 was mutated to alanine; this smaller side chain creates additional space in the binding pocket for a 2′-OH (Figure 3C). These modeling results are supported by our pre-steady state kinetic analysis of the Dpo4 Y12A mutant (37) and are consistent with the ternary crystal structures of the same mutant in complex with DNA and an incoming dNTP or rNTP (unpublished data, K. Kirouac, Z. Suo, and H. Ling).

However, the classical 'steric gate' model may not apply to every DNA polymerase. For example, crystallographic evidence suggested that X-family DNA polymerases β (38,39) and λ (40) use a protein backbone segment, rather than a large side chain discussed above, to exclude rNTPs (Figure 1E). This prediction was tested recently for human Pol λ (31). Using

site-directed mutagenesis and pre-steady state kinetic techniques, it was shown that the side chain of Y505 plays a minor role in sugar selection, thereby suggesting that the backbone segment of Y505–G508 likely governs ribonucleotide exclusion in Pol λ's active site (Figure 2). In contrast, Pol μ and terminal deoxynucleotidyl transferase (TdT), two X-family members, lack a proficient mechanism for rNTP discrimination due to a Gly residue that is encoded at the putative 'steric gate' position (Figure 1F) (16,41,42). Replacing G433 with Tyr in human Pol μ enhanced the sugar selectivity value by at least 3- to 19-fold depending on the dNTP/rNTP pair (Figure 2) (42). Taken together, either a 'steric gate' residue or a protein backbone segment plays a major role in the steric exclusion of rNTPs by a DNA polymerase or RT, which has led to an expansion of the classical steric exclusion model.

Replicative DNA polymerases usually possess 3′ → 5′ exonuclease proofreading activity; therefore, misincorporated rNMPs are potential substrates for this editing function. Studies based on wild-type (WT) Phi 29, Klenow Fragment (KF) of *Escherichia coli* DNA polymerase I, T4, and T7 DNA polymerase show that incorporated rNMPs are excised with efficiencies similar to complementary dNMPs (24,43). However, the extension of an rNMP-terminated primer by the polymerase active site of a replicative DNA polymerase is usually slow, which facilitates the excision of the rNMP moiety by the 3′ → 5′ exonuclease activity through two competing kinetic pathways: i) direct transfer of the primer strand from the polymerase active site to the exonuclease active site for editing; ii) first DNA dissociation from the polymerase active site and then the rebinding of DNA to the exonuclease active site for editing. A better understanding of how misincorporated rNMPs affect the kinetic partitioning between the polymerase and exonuclease active sites is needed, especially when yeast replicative Pols α, δ, and ε may incorporate 10,000 rNTPs during genomic replication (14,15). Overall, nucleotide discrimination at the polymerase active site is likely more important for preventing rNTP insertion than removal by the exonuclease active site. In general, both high- and low-fidelity DNA polymerases achieve overlapping sugar selectivity values, thereby reflecting that the universal mechanism of steric exclusion is conserved among the polymerase families (Table 1). However, the low-fidelity DNA polymerases (*e.g.* X- and Y-family members in Table 1) are less likely to effectively distinguish dNTPs from rNTPs than the high-fidelity polymerases (*e.g.* A- and B-family members in Table 1) (44). For example, the range of sugar selectivity values is 500-4,400,000 for the high-fidelity polymerases compared to 1.3-50,000 for the low-fidelity polymerases (Table 1). Such differences in nucleotide specificities between high- and low-fidelity DNA polymerases may be related to the overall flexibility and arrangement of their distinct active sites (Figure 1) (44-48).

Role of the flanking residues of the 'steric gate' residue on rNTP exclusion

The nucleotide binding pocket is defined by specific interactions between the active site residues and the nucleotide substrate. In addition to the side chain of a 'steric gate' residue, the backbone NH of the 'steric gate' residue or a glycine for the X-family members is within hydrogen bonding distance of the 3′-OH of an incoming nucleotide. Other active site residues are necessary to maintain the proper orientation of the nucleotide and the side chain of the 'steric gate' residue in order to achieve high sugar selectivity. For example, a highly conserved hydrophobic amino acid residue (*e.g.* I614 for *Thermus aquaticus* DNA polymerase I (*Taq*), L415 for RB69, A114 for HIV-1 RT, *etc.*), which flanks the N-terminus of the 'steric gate' residue, can form a hydrogen bond between its backbone NH and a non-bridging oxygen in the β-phosphate of a bound nucleotide for most of the polymerase families. For the A-family member *Taq*, the nucleobase is stacked and stabilized by the side chain of F667 while the side chain hydroxyl group of Y671 is hydrogen bonded to the 'steric gate' E615 (Figure 1A). Meanwhile, the Y-family member Dpo4 uses A44 to stack with the base of the incoming nucleotide and the side chain hydroxyl group of the adjacent residue

T45 to hydrogen bond with a non-bridging oxygen in the β-phosphate (Figure 1D). Overall, each network of enzyme-substrate interactions is important to effectively discriminate between rNTPs and dNTPs. Furthermore, these structural findings suggest efficient RNA synthesis is a functionality conferred by multiple residues.

rNTP incorporation and extension are more complex than a single residue model

Although the 'steric gate' residue strongly influences rNTP insertion, it does not necessarily regulate successive rNTP incorporations. The extension of an rNMP-containing primer often leads to premature termination of RNA synthesis after the addition of approximately 4 to 7 rNTPs for various enzymes with a 'steric gate' residue of reduced size (20,23,24,41,42,49). This extension problem likely originates from the suboptimal alignment of the 3′-OH due to the presence of the 2′-OH on the ribose ring or the inability of a polymerase's DNA binding cleft to accommodate the A-like helix of an RNA/DNA duplex rather than the standard B-form helix of a DNA/DNA duplex (50-54). In contrast, Dbh F12A and Dpo4 Y12A are capable of performing at least 10 and 20 rNTP insertions, respectively, without any significant pausing (28,37), a catalytic function that may be related to their flexible active site or the additional little finger subdomain of Y-family DNA polymerases which could assist the binding of an A-form helix.

Interestingly, some less obvious mutations have also been shown to relax the sugar specificity and/or to stimulate enhanced rNTP synthesis by DNA polymerases and RTs. For example, ribonucleotide incorporation was greater than WT for the following mutants: 15-fold for *Taq* A661E (55), 20- to 77- fold for *E. coli* Pol I I709F (56), 13-fold for KF F762A (20), 3-fold for human immunodeficiency virus type 1 (HIV-1) RT A114S (57), 13-fold for Vent A488L (29), and 60- to 300,000-fold for various *Taq* mutants (Figure 4) which were created using directed evolution methodologies (21,58,59). These selected point mutants discriminate less against rNTPs during incorporation, albeit some are not at the extremely low level measured for the 'steric gate' mutants (Figure 2). Nonetheless, the mutations are critical for a DNA polymerase to perform multiple rNTP incorporations.

Based on the available ternary crystal structures (3KTQ for *Taq* and 1RTD for HIV-1 RT (60,61)), side chains of the non-'steric gate' residues are 4.5 to 37 Å away from the C2′ position and are in closer proximity to the base or phosphate groups, rather than the ribose, of the incoming nucleotide (Figure 4). In addition, most of the other mutation sites do not interact directly with the DNA substrate. Together, these biochemical and structural findings suggest that other direct or indirect interactions with the rNTP substrate facilitate incorporation and elongation of an rNMP-terminated primer. Enzyme dynamics may play a prominent role in the nucleotide discrimination process, for complementary rNTP-induced conformational changes of KF are different from a correct dNTP (9,62). Stopped-flow studies on KF indicate that, compared to a correct dNTP, the rate of the conformational change from an open to closed state is reduced by ~100-fold for a complementary incoming rNTP (9). Additionally, different conformational transitions occur with mismatched dNTPs (8,9). Thus, the interrelationship between enzyme dynamics and its substrates remains an enigmatic and relatively unexplored area of research in the DNA polymerase field. Understanding the dynamics and function of other residues, both within and outside of the active site, are important for establishing a comprehensive mechanism of sugar discrimination. Altogether, to create a *bona fide* RNA polymerase from a DNA polymerase scaffold, more studies need to focus on expanding the substrate repertoire of the polymeric nucleic acid (*i.e.* RNA or DNA) rather than the incoming nucleotide (*i.e.* rNTP or dNTP).

Beyond sugar specificity: other conserved functions of the 'steric gate' residue

Besides acting as a sugar determinant, the 'steric gate' residue has been implicated in various functions, particularly lesion bypass. For each of the Y-family DNA polymerases *E. coli* Pol IV (F13V), Dbh (F12A), human Pol κ (Y112A), and *E. coli* Pol V (Y11A), the 'steric gate' residue is sometimes required for, or at least enhances, the bypass of a myriad of DNA lesions based on *in vitro* and *in vivo* results (30,63,64). Surprisingly, the 'steric gate' residue Y112 of human Pol κ controls its mutagenic potential by increasing the catalytic efficiency during extension of a mismatched primer terminus by about 400-fold (30) and by favoring the misincorporation of an oxidized nucleotide, 7,8-dihydro-8-oxo-2′-deoxyguanosine 5′-triphosphate, opposite template dA (65). In regards to polymerase fidelity, the 'steric gate' residue E710 of KF, an A-family member, is important for excluding purine-pyrimidine mismatches whereas the 'steric gate' residue F12 of Dbh, a Y-family member, maintained a relatively low fidelity similar to WT (44).

Sugar recognition at the 2′-position

To exclude rNTPs, DNA polymerases depend on two critical properties of the 2′-substituent: size and stereochemistry. Various nucleotide analogs, including the anticancer drugs cytarabine (araC) and gemcitabine (GemC), have been useful in dissecting the chemical importance of the 2′-group as well as other positions on the ribose ring during nucleotide incorporation. Nucleotide analogs containing chemical groups smaller than a hydroxyl, such as fluorine for GemC, are incorporated with efficiencies more similar to dNTPs while analogs with larger chemical groups, such as a *O*-methyl or amine, are incorporated with efficiencies similar to or worst than rNTPs (31-33,66). In addition, when the 2′-OH is pointed above the ribose ring such as an arabinonucleotide like araCTP, the different orientation of the O2′ evades the collision with the 'steric gate' residue (26,31-33,67,68). Recently, a truncated form of human Pol λ and gapped DNA was crystallized with araCMP or GemCTP as incoming nucleotides (69). The ribose of araC is bound similar to dC since the 2′-OH is directed away from the backbone COO of Y505, but for GemC, the ribose is displaced approximately 1 Å from the standard binding position so that the difluoro group does not interfere with the positioning of active site residues Y505 and N513. Despite the efficient incorporation of araCTP, the extension of this altered analog is typically more problematic than extending rCMP (68,70). Therefore, the slow extension of araCMP and GemCMP makes these anticancer drugs effective inhibitors of DNA polymerization by functioning as 'masked' chain terminators (67,70-74). In comparison, GemCTP is not a masked chain terminator for human Pol γ and human Pol η, although, the incorporation and/or extension step was less efficient compared to undamaged DNA (74,75).

Internalization of ribonucleotides into DNA: bypass and removal processes

Ribonucleotides can become embedded into genomic DNA following the successful incorporation of an rNTP opposite damaged or undamaged DNA and the subsequent step of either extension or ligation of an rNMP-terminated primer (76). For human Pol β, the incorporation efficiency of a correct dNTP onto an rNMP-terminated primer is as efficient as a dNMP-terminated primer (68). Similarly, nicked DNA with a 3′-terminal rNMP can be sealed by various DNA ligases that function in DNA repair pathways (16-18). In addition, nicked DNA containing araCMP and GemCMP, two anticancer drugs, is a substrate for human DNA ligases III/XRCC1 and I (Brown and Suo, unpublished data) (32). These events lead to the possibility of a natural or modified rNMP to persist in genomic DNA which, due to the altered structure of RNA, may interfere with future replication cycles. For example, a single rG residue within a DNA template impedes DNA replication by yeast Pol ε (14); human Pol γ can efficiently incorporate only a single dNTP with an RNA template (77). During gap-filling DNA synthesis, human Pol β inserted dCTP opposite rG with a moderate 8-fold reduction in catalytic efficiency while human Pol μ was almost non-functional with

an RNA template (16,68). Bypassing a site-specific araCMP or GemCMP embedded in a DNA template is inefficient for Pol α (70,71,73,74) and human Pol γ (75) but not human Pol η (74).

The presence of a DNA/RNA intermediate is physiologically relevant in the form of an Okazaki fragment during lagging strand DNA synthesis, therefore, cellular processes exist to recognize and to remove the inherently unstable RNA. Initiator RNA is removed by the activities of RNase H, flap endonuclease 1 (FEN1), and Pol δ (78-81). Consequently, these enzymes have been proposed to function in the removal of aberrant rNTP incorporation by DNA polymerases (15). It has been shown that the concerted nicking activity of RNase H and FEN1 can release a single rNMP from a DNA duplex, thereby generating a gap intermediate that could be processed by the base excision repair pathway (82). Alternatively, type 1 topoisomerase possesses endoribonuclease activity to excise a site-specific rNMP in DNA (83). Details on how these putative RNA-removal pathways function *in vivo* have not been elucidated. It is possible that other protein co-factors or pathways are also involved.

CONCLUDING REMARKS

Understanding the kinetic and structural mechanisms of sugar recognition is necessary in order to expand the utility of DNA polymerases in various applications. DNA polymerases are utilized for enzymatic synthesis of DNA in various applications such as polymerase chain reaction (PCR) (84,85), cDNA cloning, DNA sequencing (86), and detection of single nucleotide polymorphisms (SNPs) (87). These methods are essential experimental tools for a basic scientist and are useful diagnostic tools for a clinician that needs genomic sequence information for confirming genetic diseases, treating cancer, or overcoming drug resistance. Consequently, the enzymatic synthesis of short RNA oligonucleotides by a modified DNA polymerase is attractive because of (i) the high cost of chemical RNA synthesis, (ii) unlike methods using an RNA polymerase, modified DNA polymerases do not require a promoter sequence to be included in the PCR template, and (iii) T7 RNA polymerase cannot efficiently synthesize short RNA oligomers (*i.e.* < 50). Moreover, due to the intrinsic instability of RNA, synthesis using 2′-modified rNTPs is another future consideration because RNA composed of 2′-fluoro, 2′-*O*-methyl, 2′-*O*-methoxyethyl, and 2′,4′-bicyclic rNMPs displays greater stability, especially against nuclease-catalyzed digestion (88,89). However, one drawback for the use of a modified DNA polymerase to synthesize RNA is their inability to initiate synthesis *de novo*, thereby requiring a presynthesized primer.

The knowledge gained from sugar recognition can also be applied to designing improved nucleoside analogs for anticancer and antiviral usage. Some of the anticancer and antiviral nucleoside analogs have modified ribose structures. The design of new drugs can be accelerated with a better understanding of the mechanisms of sugar recognition employed by human DNA polymerases and viral polymerases or RTs. Nuances in their mechanisms of sugar recognition have been exploited to overcome unwanted drug toxicity and resistance. Of course, the design of nucleoside analogs requires the consideration of other enzymatic pathways, *e.g.* phosphorylation by human or viral kinases. Nonetheless, the mechanisms of sugar selectivity are of high significance for the development of anticancer and antiviral drugs, especially when specific human DNA repair and lesion bypass polymerases have been proposed to be anticancer drug targets (90).

ABBREVIATIONS

Dbh	DinB homolog of *Sulfolobus acidocaldarius*
ddNTP	2′,3′-dideoxyribonucleoside 5′-triphosphate

dNTP	2′-deoxyribonucleoside 5′-triphosphate
Dpo4	DNA polymerase IV of *Sulfolobus solfataricus*
FEN1	flap endonuclease 1
HIV-1	human immunodeficiency virus type I
KF	Klenow Fragment of *Escherichia coli* DNA polymerase I
MMLV	Moloney murine leukemia virus
Pol	DNA polymerase
rNTP	ribonucleoside 5′-triphosphate
RT	reverse transcriptase
Taq	*Thermus aquaticus* DNA polymerase I
TdT	terminal deoxynucleotidyl transferase
WT	wild type

References

1. Braithwaite DK, Ito J. Compilation, alignment, and phylogenetic relationships of DNA polymerases. Nucleic Acids Res 1993;21:787–802. [PubMed: 8451181]
2. Ohmori H, Friedberg EC, Fuchs RP, Goodman MF, Hanaoka F, Hinkle D, Kunkel TA, Lawrence CW, Livneh Z, Nohmi T, et al. The Y-family of DNA polymerases. Mol Cell 2001;8:7–8. [PubMed: 11515498]
3. Fowler JD, Suo Z. Biochemical, structural, and physiological characterization of terminal deoxynucleotidyl transferase. Chem Rev 2006;106:2092–2110. [PubMed: 16771444]
4. Garcia-Diaz M, Bebenek K. Multiple functions of DNA polymerases. CRC Crit Rev Plant Sci 2007;26:105–122. [PubMed: 18496613]
5. Steitz TA. DNA polymerases: structural diversity and common mechanisms. J Biol Chem 1999;274:17395–17398. [PubMed: 10364165]
6. Joyce CM, Benkovic SJ. DNA polymerase fidelity: kinetics, structure, and checkpoints. Biochemistry 2004;43:14317–14324. [PubMed: 15533035]
7. Rothwell PJ, Mitaksov V, Waksman G. Motions of the fingers subdomain of klentaq1 are fast and not rate limiting: implications for the molecular basis of fidelity in DNA polymerases. Mol Cell 2005;19:345–355. [PubMed: 16061181]
8. Tsai YC, Johnson KA. A new paradigm for DNA polymerase specificity. Biochemistry 2006;45:9675–9687. [PubMed: 16893169]
9. Joyce CM, Potapova O, Delucia AM, Huang X, Basu VP, Grindley ND. Fingers-closing and other rapid conformational changes in DNA polymerase I (Klenow fragment) and their role in nucleotide selectivity. Biochemistry 2008;47:6103–6116. [PubMed: 18473481]
10. Beckman JW, Wang Q, Guengerich FP. Kinetic analysis of correct nucleotide insertion by a Y-family DNA polymerase reveals conformational changes both prior to and following phosphodiester bond formation as detected by tryptophan fluorescence. J Biol Chem 2008;283:36711–36723. [PubMed: 18984592]
11. Xu C, Maxwell BA, Brown JA, Zhang L, Suo Z. Global conformational dynamics of a Y-family DNA polymerase during catalysis. PLoS Biol 2009;7:e1000225. [PubMed: 19859523]
12. Traut TW. Physiological concentrations of purines and pyrimidines. Mol Cell Biochem 1994;140:1–22. [PubMed: 7877593]
13. Ferraro P, Franzolin E, Pontarin G, Reichard P, Bianchi V. Quantitation of cellular deoxynucleoside triphosphates. Nucleic Acids Res 2010;38:e85. [PubMed: 20008099]

14. McElhinny, S.A. Nick; Watts, BE.; Kumar, D.; Watt, DL.; Lundstrom, EB.; Burgers, PM.; Johansson, E.; Chabes, A.; Kunkel, TA. Abundant ribonucleotide incorporation into DNA by yeast replicative polymerases. Proc Natl Acad Sci U S A 2010;107:4949–4954. [PubMed: 20194773]
15. McElhinny, S.A. Nick; Kumar, D.; Clark, AB.; Watt, DL.; Watts, BE.; Lundstrom, EB.; Johansson, E.; Chabes, A.; Kunkel, TA. Genome instability due to ribonucleotide incorporation into DNA. Nat Chem Biol 2010;6:774–781. [PubMed: 20729855]
16. McElhinny, S.A. Nick; Ramsden, DA. Polymerase mu is a DNA-directed DNA/RNA polymerase. Mol Cell Biol 2003;23:2309–2315. [PubMed: 12640116]
17. Pascal JM, O'Brien PJ, Tomkinson AE, Ellenberger T. Human DNA ligase I completely encircles and partially unwinds nicked DNA. Nature 2004;432:473–478. [PubMed: 15565146]
18. Zhu H, Shuman S. Bacterial nonhomologous end joining ligases preferentially seal breaks with a 3′-OH monoribonucleotide. J Biol Chem 2008;283:8331–8339. [PubMed: 18203718]
19. Joyce CM. Choosing the right sugar: how polymerases select a nucleotide substrate. Proc Natl Acad Sci U S A 1997;94:1619–1622. [PubMed: 9050827]
20. Astatke M, Ng K, Grindley ND, Joyce CM. A single side chain prevents Escherichia coli DNA polymerase I (Klenow fragment) from incorporating ribonucleotides. Proc Natl Acad Sci U S A 1998;95:3402–3407. [PubMed: 9520378]
21. Patel PH, Loeb LA. Multiple amino acid substitutions allow DNA polymerases to synthesize RNA. J Biol Chem 2000;275:40266–40272. [PubMed: 11005812]
22. Gao G, Orlova M, Georgiadis MM, Hendrickson WA, Goff SP. Conferring RNA polymerase activity to a DNA polymerase: a single residue in reverse transcriptase controls substrate selection. Proc Natl Acad Sci U S A 1997;94:407–411. [PubMed: 9012795]
23. Gardner AF, Jack WE. Determinants of nucleotide sugar recognition in an archaeon DNA polymerase. Nucleic Acids Res 1999;27:2545–2553. [PubMed: 10352184]
24. Bonnin A, Lazaro JM, Blanco L, Salas M. A single tyrosine prevents insertion of ribonucleotides in the eukaryotic-type phi29 DNA polymerase. J Mol Biol 1999;290:241–251. [PubMed: 10388570]
25. Cases-Gonzalez CE, Gutierrez-Rivas M, Menendez-Arias L. Coupling ribose selection to fidelity of DNA synthesis. The role of Tyr-115 of human immunodeficiency virus type 1 reverse transcriptase. J Biol Chem 2000;275:19759–19767. [PubMed: 10748215]
26. Yang G, Franklin M, Li J, Lin TC, Konigsberg W. A conserved Tyr residue is required for sugar selectivity in a Pol alpha DNA polymerase. Biochemistry 2002;41:10256–10261. [PubMed: 12162740]
27. Beck J, Vogel M, Nassal M. dNTP versus NTP discrimination by phenylalanine 451 in duck hepatitis B virus P protein indicates a common structure of the dNTP-binding pocket with other reverse transcriptases. Nucleic Acids Res 2002;30:1679–1687. [PubMed: 11917030]
28. DeLucia AM, Grindley ND, Joyce CM. An error-prone family Y DNA polymerase (DinB homolog from Sulfolobus solfataricus) uses a 'steric gate' residue for discrimination against ribonucleotides. Nucleic Acids Res 2003;31:4129–4137. [PubMed: 12853630]
29. Gardner AF, Joyce CM, Jack WE. Comparative kinetics of nucleotide analog incorporation by vent DNA polymerase. J Biol Chem 2004;279:11834–11842. [PubMed: 14699133]
30. Niimi N, Sassa A, Katafuchi A, Gruz P, Fujimoto H, Bonala RR, Johnson F, Ohta T, Nohmi T. The steric gate amino acid tyrosine 112 is required for efficient mismatched-primer extension by human DNA polymerase kappa. Biochemistry 2009;48:4239–4246. [PubMed: 19341290]
31. Brown JA, Fiala KA, Fowler JD, Sherrer SM, Newmister SA, Duym WW, Suo Z. A Novel Mechanism of Sugar Selection Utilized by a Human X-Family DNA Polymerase. J Mol Biol 2010;395:282–290. [PubMed: 19900463]
32. Gowda, A.S. Prakasha; Polizzi, JM.; Eckert, KA.; Spratt, TE. Incorporation of gemcitabine and cytarabine into DNA by DNA polymerase beta and ligase III/XRCC1. Biochemistry 2010;49:4833–4840. [PubMed: 20459144]
33. Brown JA, Fowler JD, Suo Z. Kinetic Basis of Nucleotide Selection Employed by a Protein Template-Dependent DNA Polymerase. Biochemistry 2010;49:5504–5510. [PubMed: 20518555]
34. Vaisman A, Ling H, Woodgate R, Yang W. Fidelity of Dpo4: effect of metal ions, nucleotide selection and pyrophosphorolysis. Embo J 2005;24:2957–2967. [PubMed: 16107880]

35. Thoden JB, Holden HM, Firestine SM. Structural analysis of the active site geometry of N5-carboxyaminoimidazole ribonucleotide synthetase from Escherichia coli. Biochemistry 2008;47:13346–13353. [PubMed: 19053251]
36. Guex N, Peitsch MC. SWISS-MODEL and the Swiss-PdbViewer: an environment for comparative protein modeling. Electrophoresis 1997;18:2714–2723. http://www.expasy.org/spdbv/. [PubMed: 9504803]
37. Sherrer SM, Beyer DC, Xia CX, Fowler JD, Suo Z. Kinetic Basis of Sugar Selection by a Y-Family DNA Polymerase from Sulfolobus solfataricus P2. Biochemistry 2010;49:10179–10186. [PubMed: 20973506]
38. Pelletier H, Sawaya MR, Kumar A, Wilson SH, Kraut J. Structures of ternary complexes of rat DNA polymerase beta, a DNA template-primer, and ddCTP. Science 1994;264:1891–1903. [PubMed: 7516580]
39. Sawaya MR, Prasad R, Wilson SH, Kraut J, Pelletier H. Crystal structures of human DNA polymerase beta complexed with gapped and nicked DNA: evidence for an induced fit mechanism. Biochemistry 1997;36:11205–11215. [PubMed: 9287163]
40. Garcia-Diaz M, Bebenek K, Krahn JM, Kunkel TA, Pedersen LC. A closed conformation for the Pol lambda catalytic cycle. Nat Struct Mol Biol 2005;12:97–98. [PubMed: 15608652]
41. Boule JB, Rougeon F, Papanicolaou C. Terminal deoxynucleotidyl transferase indiscriminately incorporates ribonucleotides and deoxyribonucleotides. J Biol Chem 2001;276:31388–31393. [PubMed: 11406636]
42. Ruiz JF, Juarez R, Garcia-Diaz M, Terrados G, Picher AJ, Gonzalez-Barrera S, de Henestrosa A.R. Fernandez, Blanco L. Lack of sugar discrimination by human Pol mu requires a single glycine residue. Nucleic Acids Res 2003;31:4441–4449. [PubMed: 12888504]
43. Lin TC, Wang CX, Joyce CM, Konigsberg WH. 3′-5′ Exonucleolytic activity of DNA polymerases: structural features that allow kinetic discrimination between ribo- and deoxyribonucleotide residues. Biochemistry 2001;40:8749–8755. [PubMed: 11467934]
44. DeLucia AM, Chaudhuri S, Potapova O, Grindley ND, Joyce CM. The properties of steric gate mutants reveal different constraints within the active sites of Y-family and A-family DNA polymerases. J Biol Chem 2006;281:27286–27291. [PubMed: 16831866]
45. Ling H, Boudsocq F, Woodgate R, Yang W. Crystal structure of a Y-family DNA polymerase in action: a mechanism for error-prone and lesion-bypass replication. Cell 2001;107:91–102. [PubMed: 11595188]
46. Mizukami S, Kim TW, Helquist SA, Kool ET. Varying DNA base-pair size in subangstrom increments: evidence for a loose, not large, active site in low-fidelity Dpo4 polymerase. Biochemistry 2006;45:2772–2778. [PubMed: 16503632]
47. Moon AF, Garcia-Diaz M, Batra VK, Beard WA, Bebenek K, Kunkel TA, Wilson SH, Pedersen LC. The X family portrait: structural insights into biological functions of X family polymerases. DNA Repair (Amst) 2007;6:1709–1725. [PubMed: 17631059]
48. McCulloch SD, Kunkel TA. The fidelity of DNA synthesis by eukaryotic replicative and translesion synthesis polymerases. Cell Res 2008;18:148–161. [PubMed: 18166979]
49. Liu S, Goff SP, Gao G. Gln(84) of moloney murine leukemia virus reverse transcriptase regulates the incorporation rates of ribonucleotides and deoxyribonucleotides. FEBS Lett 2006;580:1497–1501. [PubMed: 16466720]
50. Hall KB, McLaughlin LW. Thermodynamic and structural properties of pentamer DNA.DNA, RNA.RNA, and DNA.RNA duplexes of identical sequence. Biochemistry 1991;30:10606–10613. [PubMed: 1931983]
51. Egli M, Usman N, Rich A. Conformational influence of the ribose 2′-hydroxyl group: crystal structures of DNA-RNA chimeric duplexes. Biochemistry 1993;32:3221–3237. [PubMed: 7681688]
52. Fedoroff O, Salazar M, Reid BR. Structure of a DNA:RNA hybrid duplex. Why RNase H does not cleave pure RNA. J Mol Biol 1993;233:509–523. [PubMed: 8411159]
53. Ban C, Ramakrishnan B, Sundaralingam M. A single 2′-hydroxyl group converts B-DNA to A-DNA. Crystal structure of the DNA-RNA chimeric decamer duplex d(CCGGC)r(G)d(CCGG) with

a novel intermolecular G-C base-paired quadruplet. J Mol Biol 1994;236:275–285. [PubMed: 7508984]

54. Wahl MC, Sundaralingam M. B-form to A-form conversion by a 3′-terminal ribose: crystal structure of the chimera d(CCACTAGTG)r(G). Nucleic Acids Res 2000;28:4356–4363. [PubMed: 11058136]
55. Ogawa M, Tosaka A, Ito Y, Yoshida S, Suzuki M. Enhanced ribonucleotide incorporation by an O-helix mutant of Thermus aquaticus DNA polymerase I. Mutat Res 2001;485:197–207. [PubMed: 11267831]
56. Shinkai A, Patel PH, Loeb LA. The conserved active site motif A of Escherichia coli DNA polymerase I is highly mutable. J Biol Chem 2001;276:18836–18842. [PubMed: 11278911]
57. Cases-Gonzalez CE, Menendez-Arias L. Nucleotide specificity of HIV-1 reverse transcriptases with amino acid substitutions affecting Ala-114. Biochem J 2005;387:221–229. [PubMed: 15548134]
58. Xia G, Chen L, Sera T, Fa M, Schultz PG, Romesberg FE. Directed evolution of novel polymerase activities: mutation of a DNA polymerase into an efficient RNA polymerase. Proc Natl Acad Sci U S A 2002;99:6597–6602. [PubMed: 12011423]
59. Ong JL, Loakes D, Jaroslawski S, Too K, Holliger P. Directed evolution of DNA polymerase, RNA polymerase and reverse transcriptase activity in a single polypeptide. J Mol Biol 2006;361:537–550. [PubMed: 16859707]
60. Li Y, Korolev S, Waksman G. Crystal structures of open and closed forms of binary and ternary complexes of the large fragment of Thermus aquaticus DNA polymerase I: structural basis for nucleotide incorporation. Embo J 1998;17:7514–7525. [PubMed: 9857206]
61. Huang H, Chopra R, Verdine GL, Harrison SC. Structure of a covalently trapped catalytic complex of HIV-1 reverse transcriptase: implications for drug resistance. Science 1998;282:1669–1675. [PubMed: 9831551]
62. Datta K, Johnson NP, von Hippel PH. DNA conformational changes at the primer-template junction regulate the fidelity of replication by DNA polymerase. Proc Natl Acad Sci U S A 2010;107:17980–17985. [PubMed: 20921373]
63. Jarosz DF, Godoy VG, Delaney JC, Essigmann JM, Walker GC. A single amino acid governs enhanced activity of DinB DNA polymerases on damaged templates. Nature 2006;439:225–228. [PubMed: 16407906]
64. Shurtleff BW, Ollivierre JN, Tehrani M, Walker GC, Beuning PJ. Steric gate variants of UmuC confer UV hypersensitivity on Escherichia coli. J Bacteriol 2009;191:4815–4823. [PubMed: 19482923]
65. Katafuchi A, Sassa A, Niimi N, Gruz P, Fujimoto H, Masutani C, Hanaoka F, Ohta T, Nohmi T. Critical amino acids in human DNA polymerases eta and kappa involved in erroneous incorporation of oxidized nucleotides. Nucleic Acids Res 2010;38:859–867. [PubMed: 19939936]
66. Richardson FC, Kuchta RD, Mazurkiewicz A, Richardson KA. Polymerization of 2′-fluoro- and 2′-O-methyl-dNTPs by human DNA polymerase alpha, polymerase gamma, and primase. Biochem Pharmacol 2000;59:1045–1052. [PubMed: 10704933]
67. Kuchta RD, Ilsley D, Kravig KD, Schubert S, Harris B. Inhibition of DNA primase and polymerase alpha by arabinofuranosylnucleoside triphosphates and related compounds. Biochemistry 1992;31:4720–4728. [PubMed: 1581321]
68. Cavanaugh NA, Beard WA, Wilson SH. DNA polymerase {beta} ribonucleotide discrimination: insertion, misinsertion, extension, and coding. J Biol Chem. 2010
69. Garcia-Diaz M, Murray MS, Kunkel TA, Chou KM. Interaction between DNA Polymerase lambda and anticancer nucleoside analogs. J Biol Chem 2010;285:16874–16879. [PubMed: 20348107]
70. Harrington C, Perrino FW. The effects of cytosine arabinoside on RNA-primed DNA synthesis by DNA polymerase alpha-primase. J Biol Chem 1995;270:26664–26669. [PubMed: 7592892]
71. Mikita T, Beardsley GP. Functional consequences of the arabinosylcytosine structural lesion in DNA. Biochemistry 1988;27:4698–4705. [PubMed: 2458756]
72. Huang P, Chubb S, Hertel LW, Grindey GB, Plunkett W. Action of 2′,2′-difluorodeoxycytidine on DNA synthesis. Cancer Res 1991;51:6110–6117. [PubMed: 1718594]

73. Richardson KA, Vega TP, Richardson FC, Moore CL, Rohloff JC, Tomkinson B, Bendele RA, Kuchta RD. Polymerization of the triphosphates of AraC, 2′,2′-difluorodeoxycytidine (dFdC) and OSI-7836 (T-araC) by human DNA polymerase alpha and DNA primase. Biochem Pharmacol 2004;68:2337–2346. [PubMed: 15548380]
74. Chen YW, Cleaver JE, Hanaoka F, Chang CF, Chou KM. A novel role of DNA polymerase eta in modulating cellular sensitivity to chemotherapeutic agents. Mol Cancer Res 2006;4:257–265. [PubMed: 16603639]
75. Fowler JD, Brown JA, Johnson KA, Suo Z. Kinetic investigation of the inhibitory effect of gemcitabine on DNA polymerization catalyzed by human mitochondrial DNA polymerase. J Biol Chem 2008;283:15339–15348. [PubMed: 18378680]
76. Bergoglio V, Ferrari E, Hubscher U, Cazaux C, Hoffmann JS. DNA polymerase beta can incorporate ribonucleotides during DNA synthesis of undamaged and CPD-damaged DNA. J Mol Biol 2003;331:1017–1023. [PubMed: 12927538]
77. Lee HR, Johnson KA. Fidelity and processivity of reverse transcription by the human mitochondrial DNA polymerase. J Biol Chem 2007;282:31982–31989. [PubMed: 17711845]
78. Bambara RA, Murante RS, Henricksen LA. Enzymes and reactions at the eukaryotic DNA replication fork. J Biol Chem 1997;272:4647–4650. [PubMed: 9081985]
79. Rossi ML, Purohit V, Brandt PD, Bambara RA. Lagging strand replication proteins in genome stability and DNA repair. Chem Rev 2006;106:453–473. [PubMed: 16464014]
80. Burgers PM. Polymerase dynamics at the eukaryotic DNA replication fork. J Biol Chem 2009;284:4041–4045. [PubMed: 18835809]
81. Cerritelli SM, Crouch RJ. Ribonuclease H: the enzymes in eukaryotes. FEBS J 2009;276:1494–1505. [PubMed: 19228196]
82. Rydberg B, Game J. Excision of misincorporated ribonucleotides in DNA by RNase H (type 2) and FEN-1 in cell-free extracts. Proc Natl Acad Sci U S A 2002;99:16654–16659. [PubMed: 12475934]
83. Sekiguchi J, Shuman S. Site-specific ribonuclease activity of eukaryotic DNA topoisomerase I. Mol Cell 1997;1:89–97. [PubMed: 9659906]
84. Saiki RK, Scharf S, Faloona F, Mullis KB, Horn GT, Erlich HA, Arnheim N. Enzymatic amplification of beta-globin genomic sequences and restriction site analysis for diagnosis of sickle cell anemia. Science 1985;230:1350–1354. [PubMed: 2999980]
85. Saiki RK, Gelfand DH, Stoffel S, Scharf SJ, Higuchi R, Horn GT, Mullis KB, Erlich HA. Primer-directed enzymatic amplification of DNA with a thermostable DNA polymerase. Science 1988;239:487–491. [PubMed: 2448875]
86. Sanger F, Nicklen S, Coulson AR. DNA sequencing with chain-terminating inhibitors. Proc Natl Acad Sci U S A 1977;74:5463–5467. [PubMed: 271968]
87. Sarkar G, Yoon HS, Sommer SS. Dideoxy fingerprinting (ddE): a rapid and efficient screen for the presence of mutations. Genomics 1992;13:441–443. [PubMed: 1612601]
88. Monia BP, Lesnik EA, Gonzalez C, Lima WF, McGee D, Guinosso CJ, Kawasaki AM, Cook PD, Freier SM. Evaluation of 2′-modified oligonucleotides containing 2′-deoxy gaps as antisense inhibitors of gene expression. J Biol Chem 1993;268:14514–14522. [PubMed: 8390996]
89. Bennett CF, Swayze EE. RNA targeting therapeutics: molecular mechanisms of antisense oligonucleotides as a therapeutic platform. Annu Rev Pharmacol Toxicol 2010;50:259–293. [PubMed: 20055705]
90. Maga G, Hubscher U. Repair and translesion DNA polymerases as anticancer drug targets. Anticancer Agents Med Chem 2008;8:431–447. [PubMed: 18473728]

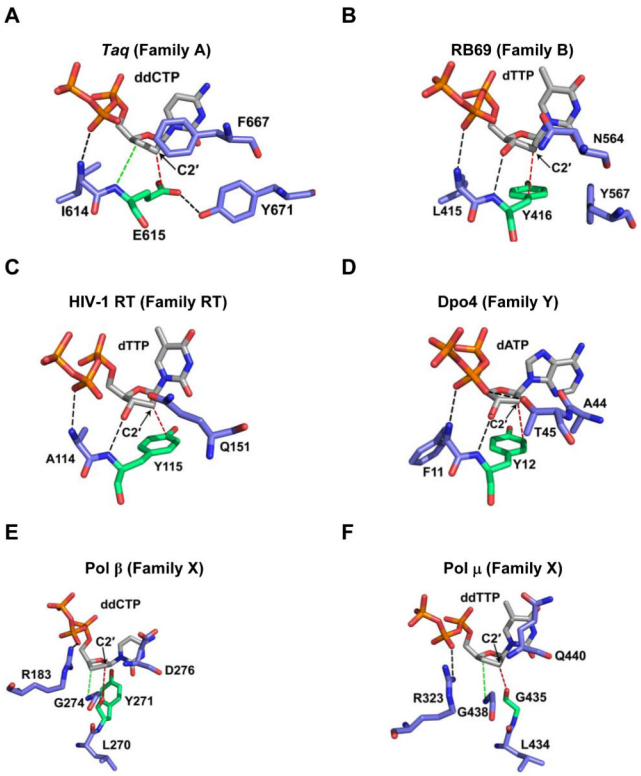

Figure 1.

Structural basis for ribonucleotide exclusion. The ‘steric gate’ residues (green sticks) and other nearby active site residues (lavendar sticks) are shown with the incoming nucleotide (gray sticks) for (A) *Taq* (PDB 3KTQ), (B) RB69 (PDB 1IG9), (C) HIV-1 RT (PDB 1RTD), (D) Dpo4 (PDB 2AGQ), (E) human Pol β (PDB 1BPY), and (F) mouse Pol μ (PDB 2IHM). The C2′ position is indicated using an arrow for each nucleotide. The shortest distance between the ‘steric gate’ and C2′ position is indicated with a red dashed line. Hydrogen bonding interactions are shown as a black dashed line while potential hydrogen bonds with the missing 3′-OH are shown as a green dashed line.

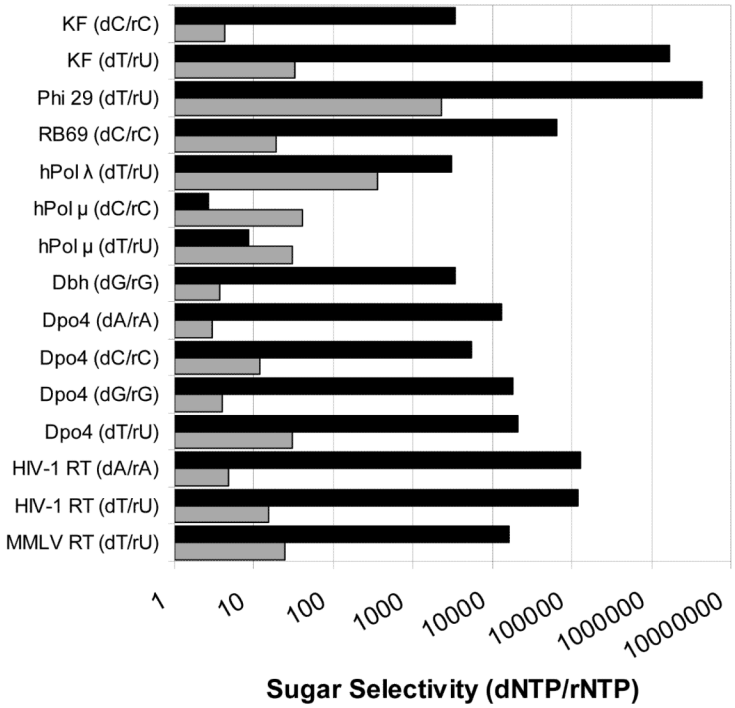

Figure 2.

Measurements of sugar selectivity for ‘steric gate’ mutants. The sugar selectivity values of WT (dark bars) and mutant (gray bars) DNA polymerases and RTs were obtained from the references listed in Table 1. The mutations are as follows: E710A for KF, Y254V for Phi 29, Y416A for RB69, Y505A for hPol λ, G433Y for hPol μ, F12A for Dbh, Y12A for Dpo4, Y115A for HIV-1 RT, and F155V for MMLV RT. The incoming dNTP and rNTP pair are indicated in parenthesis.

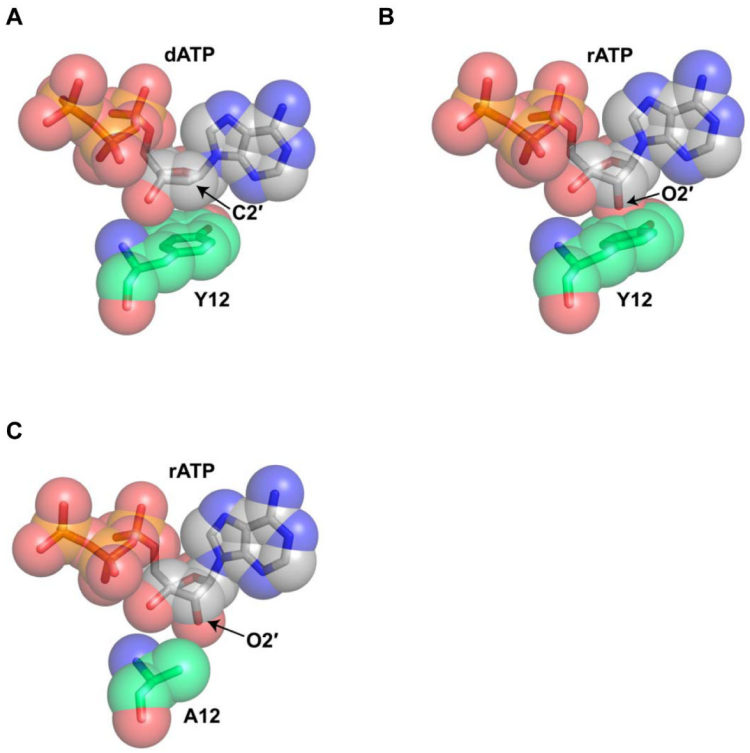

Figure 3.

Structural models of a ribonucleotide in the active site of Dpo4. The ‘steric gate’ residue (green sticks) and incoming nucleotide (gray sticks) are shown for (A) WT Dpo4 with dATP (PDB 2AGQ), (B) WT Dpo4 with rATP, and (C) Dpo4 Y12A with rATP. The ribose ring of rATP in (B and C) is from PDB 3ETH while the side chain of Y12 is from PDB 2AGQ and was replaced with Ala in (C) using SwissPDB Viewer (36). The 2′ position is indicated by an arrow.

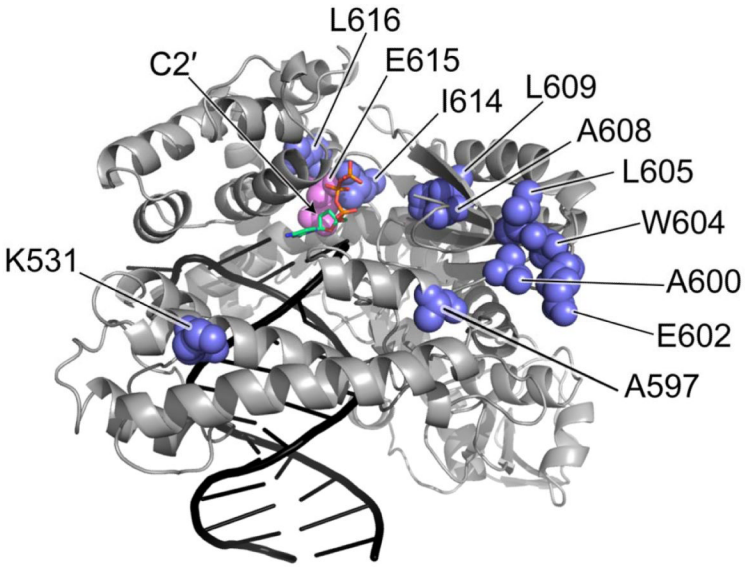

Figure 4.

Mutations mapped onto the crystal structure of a truncated form of *Taq* (PDB 3KTQ). Residues that were mutated (blue space-filling models) are labeled on the ternary complex of *Taq* (gray), DNA (black), and ddNTP (green sticks). The ‘steric gate’ residue E615 is in pink and the C2′ position is identified by an arrow.

Table 1

Measurements of sugar selectivity values for various DNA polymerases and RTs.

Polymerase Family	DNA Polymerase or RT	Sugar Selectivity[a]	Method	Reference
A	*E. coli* KF (E710)	3,100 – 1,700,000	Pre-steady state and steady state	(20,21)
	Taq (E615)	82,000 – 1,600,000	Steady state	(21,55)
	Human Pol γ (E895)	1,000	Steady state	(66)
B	Phi 29 DNA polymerase (Y254)	4,400,000	Pre-steady state	(24)
	RB69 (Y416)	64,000	Pre-steady state	(26)
	Vent (Y412)	2,000 – 10,000	Steady state and pre-steady state	(21,29)
	Bovine Pol α (Y865)	20,000	Steady state	(67)
	Human Pol α (Y865)	500	Steady state	(66)
	Yeast Pol δ (Y613)	13,000 – 1,700,000	Primer extension and steady state	(14)
X	Rat Pol β (Y271)	2,000 – 6,000	Steady state and pre-steady state	(16,32)
	Human Pol β (Y271)	8,000	Steady state	(68)
	Human Pol λ (Y505)	3,000 – 50,000	Pre-steady state	(31)
	Human Pol μ (G433)	1.3 – 11	Steady state and Primer extension	(16,42)
	Human TdT (G448)	2.6 – 8.9	Steady state	(16)
	Mouse TdT (G449)	2.0 – 4.9	Steady state and primer extension	(41)
Y	Dbh (F12)	3,400	Pre-steady state	(26)
	Dpo4 (Y12)	5,500 – 20,500	Pre-steady state	(37)
	Human Rev1 (F428)	280	Pre-steady state	(33)
RT	HIV-1 RT (Y115)	42,000 – 130,000	Steady state	(25,57)
	MMLV RT (F155)	1,100 – 21,000	Steady state	(21,22)

[a] Calculated as dNTP incorporation/rNTP incorporation.